Cell, Vol. 116, 39–50, January 9, 2004, Copyright ©2004 by Cell Press

Structural Basis for FEN-1 Substrate Specificity and PCNA-Mediated Activation in DNA Replication and Repair

Brian R. Chapados,[1,3] David J. Hosfield,[1,3,4] Seungil Han,[1,5] Junzhuan Qiu,[2] Biana Yelent,[1,6] Binghui Shen,[2] and John A. Tainer[1,*]
[1]Department of Molecular Biology
and Skaggs Institute for Chemical Biology
The Scripps Research Institute
La Jolla, California 92122
[2]Division of Molecular Medicine
City of Hope National Medical Center and Beckman Research Institute
Duarte, California 91010

Summary

Flap EndoNuclease-1 (FEN-1) and the processivity factor proliferating cell nuclear antigen (PCNA) are central to DNA replication and repair. To clarify the molecular basis of FEN-1 specificity and PCNA activation, we report here structures of FEN-1:DNA and PCNA: FEN-1-peptide complexes, along with fluorescence resonance energy transfer (FRET) and mutational results. FEN-1 binds the unpaired 3′ DNA end (3′ flap), opens and kinks the DNA, and promotes conformational closing of a flexible helical clamp to facilitate 5′ cleavage specificity. Ordering of unstructured C-terminal regions in FEN-1 and PCNA creates an intermolecular β sheet interface that directly links adjacent PCNA and DNA binding regions of FEN-1 and suggests how PCNA stimulates FEN-1 activity. The DNA and protein conformational changes, composite complex structures, FRET, and mutational results support enzyme-PCNA alignments and a kinked DNA pivot point that appear suitable to coordinate rotary handoffs of kinked DNA intermediates among enzymes localized by the three PCNA binding sites.

Introduction

*F*lap *E*ndo*N*uclease-1 (FEN-1) is a structure-specific nuclease that is central to both DNA replication and repair processes. During DNA replication and repair, a complex that includes both FEN-1 and the "sliding clamp" accessory protein proliferating cell nuclear antigen (PCNA) removes RNA primers or damaged DNA, generating a product for ligation by DNA ligase I (Bambara et al., 1997; Maga et al., 2001; Matsumoto, 2001). Several lines of evidence underscore the importance of FEN-1 activity in DNA replication and repair pathways. FEN-1 homozygous knockouts are lethal in mice, and mice heterozygous for functional FEN-1 (FEN-1/null) exhibit accelerated tumor growth (Kucherlapati et al., 2002). Deletions of FEN-1 in *Saccharomyces cerevisiae* (*rad27*) cause replication and repair defects, including increased sensitivity to UV light and chemical mutagens, genomic instability, increased tri-nucleotide repeat expansion, and destabilization of telomeric repeats (reviewed in Henneke et al., 2003). These data highlight the importance of FEN-1 function in cells and make FEN-1 a potential cancer susceptibility gene (Henneke et al., 2003).

The FEN-1 class of structure-specific 5′ nucleases occurs in all domains of life (Harrington and Lieber, 1994; Lieber, 1997; Shen et al., 1998). Unlike endonucleases that recognize a specific DNA sequence, FEN-1 recognizes a specific DNA structure, independent of the DNA sequence. Specifically, FEN-1 and related 5′ nucleases recognize a branched DNA structure consisting of a single unpaired 3′ nucleotide (3′ flap) overlapping with a variable length region of 5′ single-stranded DNA (5′ flap) (Kaiser et al., 1999; Kao et al., 2002). This "double-flap" or "overlap-flap" structure results from DNA polymerase activity that displaces damaged DNA or RNA creating a ssDNA 5′ flap. The newly synthesized DNA and the displaced region compete for base pairing with the template strand, resulting in the formation of the double-flap structure (Reynaldo et al., 2000). FEN-1 cleaves this substrate after the first base pair preceding the 5′ flap to remove the ssDNA 5′ flap and create a nicked DNA product (Kaiser et al., 1999; Kao et al., 2002; Xie et al., 2001).

The dramatic increase in FEN-1 cleavage specificity for the double-flap structure suggests that FEN-1 specifically binds to the 3′ flap (Kaiser et al., 1999). Although several structures of FEN-1 homologs exist (Ceska et al., 1996; Hosfield et al., 1998b; Hwang et al., 1998; Kim et al., 1995; Matsui et al., 2002; Mueser et al., 1996), a specific binding site for the 3′ flap has not been identified. Biochemical results also suggest that conformational changes in flexible loop regions are required for catalysis (Kim et al., 2001; Storici et al., 2002). However, in the absence of structural information on FEN-1 and DNA conformational changes, efforts to model FEN-1 interactions with DNA cannot account for the structure-specific activity observed in biochemical assays (Allawi et al., 2003; Ceska et al., 1996; Dervan et al., 2002; Hosfield et al., 1998b; Hwang et al., 1998).

In cells, FEN-1 forms a complex with PCNA, which exists as a ring-shaped homotrimer in solution (Krishna et al., 1994; Yao et al., 1996). PCNA is loaded onto DNA in an ATP-dependent reaction catalyzed by replication factor C (RF-C) (Mossi and Hubscher, 1998). After loading, PCNA encircles dsDNA and can slide freely along it (Gulbis et al., 1996; Krishna et al., 1994). In this way, PCNA can act as a molecular adaptor or "sliding clamp" that localizes bound proteins to DNA.

FEN-1 binds to PCNA through a conserved consensus motif (reviewed in Warbrick, 1998). Crystal structures of peptides derived from $p21^{waf1/cip1}$ and other proteins

*Correspondence: jat@scripps.edu
[3]These authors contributed equally to the work.
[4]Present Address: Syrrx Inc., 10410 Science Center Drive, San Diego, California 92121.
[5]Present Address: Pfizer Global Research and Development, Exploratory Medicinal Sciences (EMS), MS4039, Core Technology Group, Eastern Point Road, Groton, Connecticut 06340.
[6]Present Address: Cancer Research Laboratory and Division of Immunology, Department of Molecular and Cell Biology, 465 Life Science Addition, University of California, Berkeley, California 94720.

bound to PCNA show that half of the consensus PCNA binding motif adopts a helical conformation, placing the conserved hydrophobic residues (LXXFF) on the same face of the helix. This structure facilitates interactions with a hydrophobic pocket on the PCNA surface formed by residues in the interdomain connecting loop of PCNA (Gulbis et al., 1996; Matsumiya et al., 2002; Shamoo and Steitz, 1999). The conservation of the PCNA binding consensus motif suggests a generic way in which several different enzymes can bind to PCNA.

PCNA stimulates FEN-1 activity by up to 50-fold in vitro (Frank et al., 2001; Gomes and Burgers, 2000; Jonsson et al., 1998; Li et al., 1995; Tom et al., 2000). Even when all residues of the PCNA binding motif are mutated to alanine, preventing the known hydrophobic interaction, PCNA still stimulates FEN-1 activity (Frank et al., 2001). Furthermore, when PCNA is loaded onto DNA by RF-C, the C terminus of PCNA mediates interactions with FEN-1 (Gomes and Burgers, 2000). These results suggest that interactions with the C terminus of PCNA either involve FEN-1 residues located outside the currently defined PCNA binding motif or are somehow independent of the amino acid sequence.

Current knowledge of FEN-1 interactions with DNA and PCNA therefore raises three critical questions: (1) How does FEN-1 recognize the DNA 3′ flap? (2) How does recognition of the 3′ flap aid structure-specific catalysis? (3) How does FEN-1 interaction with PCNA increase FEN-1 activity? Here, we address these key questions by providing cocrystal structures of *Archaeoglobus fulgidus* FEN-1 bound to DNA and of two FEN-1 peptides bound to *A. fulgidus* PCNA, coupled with fluorescence energy transfer (FRET), activity, and mutational analyses.

Results

Structure of FEN-1 Bound to DNA

To characterize FEN-1 interactions with the DNA 3′ flap, we determined the structure of *Archaeoglobus fulgidus* FEN-1 bound to the 3′ upstream portion of a double-flap DNA substrate (Figures 1A–1C) by multi-wavelength anomalous dispersion (MAD) with seleno-methionine substituted FEN-1 (Supplemental Table S1 at http://www.cell.com/cgi/content/full/116/1/39/DC1). We obtained two different crystal forms, which diffracted to 2.5 Å and 2.0 Å resolution. In the two structures, the overall conformation of FEN-1 is similar, with 0.52 Å^2 root mean square deviations (rmsd) for all aligned Cα atoms. The enzyme architecture consists of a mostly parallel six-stranded β sheet surrounded on both sides by α helices that create a prominent groove, housing the enzyme active site (Figure 1B) and resembling other FEN-1 structures.

DNA binding is mediated by residues conserved in all known FEN-1 homologs (Figure 1D). These residues emanate from two pairs of α helices (α2, α3 and α14, α15) and the two loops connecting these helical pairs (α2-α3 and α14-α15; Figures 1B and 1D). In addition, the 3′ flap and associated double-stranded DNA binds in the same binding site in both structures. In experiments designed to obtain crystals of FEN-1 bound to an intact double-flap DNA substrate, we consistently trapped this same complex. The structural stability of this product complex suggests that it represents a stable intermediate in the replication and repair process.

A Unique Binding Site for the 3′ Flap

Both structures of the FEN-1:DNA complex reveal the same binding site for a 3′ flap and associated dsDNA, situated ~25 Å away from the nuclease active site (Figure 1B). Specific contacts to DNA minor groove and backbone atoms on both strands anchor the 3′ flap (G1: Figures 1C and 2A–2E) in a small pocket that sterically blocks binding of additional nucleotides (Figure 2C). Hydrophobic packing and hydrogen bonding interactions with the 3′ terminal sugar (of G1, Figure 2C), but not the associated base, allow sequence-independent recognition of 3′ nucleotides, consistent with the role of FEN-1 as a structure-specific endonuclease. The 3′ flap contributes ~36% (~350 Å^2) of the 970 Å^2 of molecular surface area buried upon FEN-1 binding to the dsDNA, suggesting that 3′ flap binding contributes significantly to FEN-1 substrate affinity.

FEN-1 makes significant hydrophobic interactions with DNA that wedge open and stabilize the bound dsDNA (Figure 2A). The interface involves the tight packing of a surface-exposed "hydrophobic wedge" (formed by α3 residues Phe35, Ile38, and Ile39 and α2-α3 loop residue Leu47) with the terminal DNA base pair (G2:C15) (Figures 1C and 2A). DNA binding is further stabilized by α3 and α15 residues that hydrogen bond with the phosphate backbone of dsDNA (Figure 2B).

To test the functional importance of the structurally defined DNA 3′ flap binding site, we tested the activity of designed mutants for key residues. Mutation of conserved interface residue Thr55 to Phe, expected to severely disrupt the binding pocket (Figures 1C and 2C), decreased FEN-1 activity at least 100-fold (Figure 2F). In addition, mutation of Arg64 to Ala, expected to disrupt hydrogen bonding to the dsDNA backbone, similarly decreased FEN-1 activity (Figure 2F). Moreover, the importance of hydrogen bonding to the 3′-hydroxyl is validated by the ~10-fold decrease in activity for 3′ flaps containing dideoxynucleotides (Kaiser et al., 1999). These results are consistent with gel shift experiments showing that FEN-1 has a significantly higher affinity for double-flap substrates compared to substrates lacking a 3′ flap (Friedrich-Heineken et al., 2003).

FEN-1 interactions with the 3′ flap and associated DNA do not depend on the identity of the bases, but instead require that the substrate adopt a specific structure. The direct interactions between the hydrophobic wedge and the 3′ flap observed in the FEN-1:DNA crystal structures interrupt the DNA helix, likely preventing a continuation of linear DNA conformation and separating the 5′ flap and associated duplex away from the 3′ flap. The identification of the hydrophobic wedge and the 3′ flap binding site, as well as their location ~25 Å from the active site, suggest that upon binding to FEN-1, the DNA substrate undergoes considerable conformational changes that originate at the flap junction.

Coupling 3′ Flap Binding to 5′ Flap Cleavage

Comparison of the FEN-1:DNA complex to FEN-1 structures determined without DNA (Hosfield et al., 1998b;

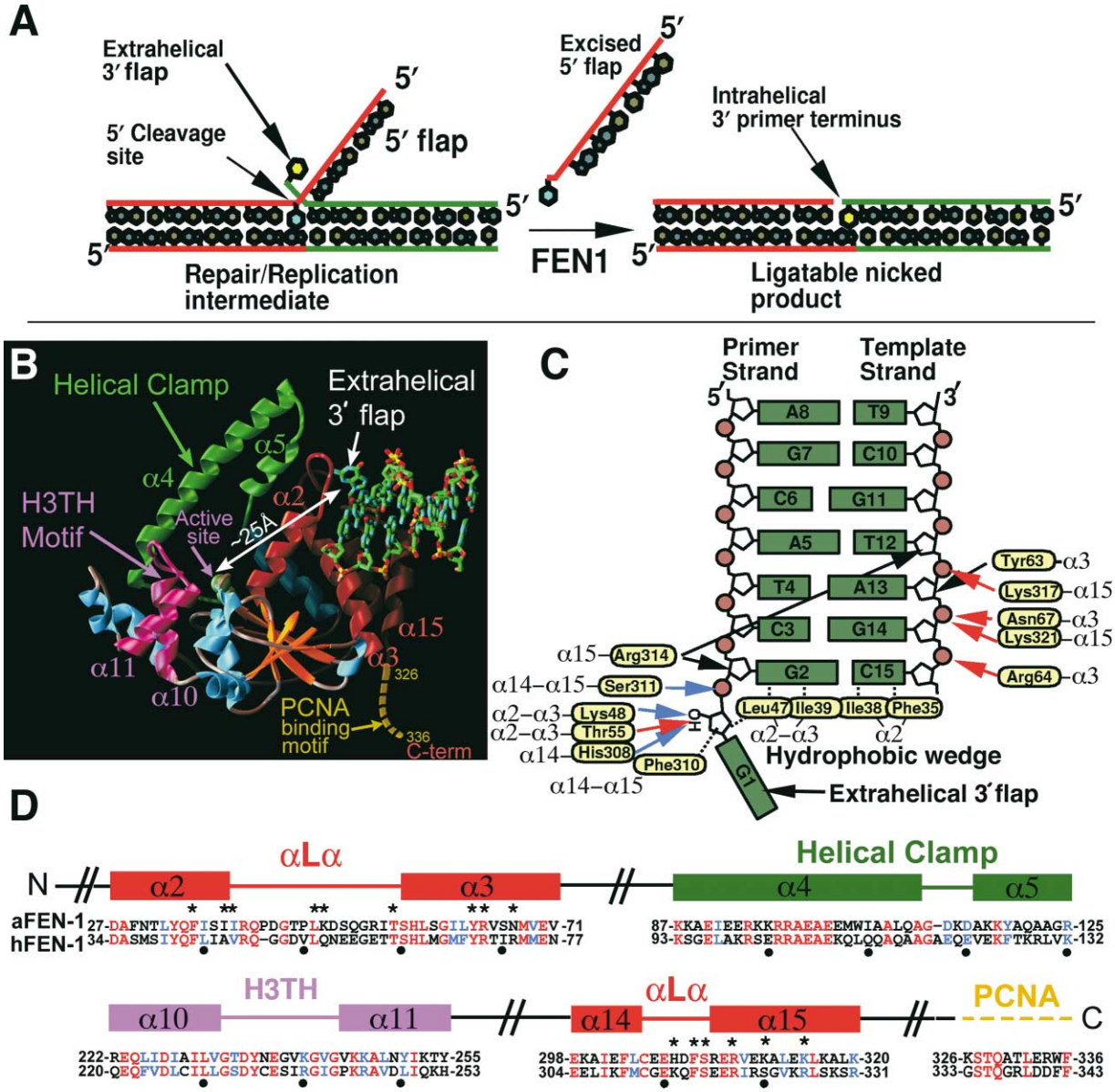

Figure 1. FEN-1 3′ Flap Recognition and Substrate Specificity

(A) The optimal double-flap substrate for FEN-1 includes both an upstream DNA duplex (green) containing an unpaired 3′ single-nucleotide 3′ flap (yellow) and a downstream DNA duplex (red) containing the 5′ polynucleotide flap and scissile phosphate that is cleaved by the enzyme.

(B) Overall structure of the aFEN-1:DNA complex, showing the locations of the upstream DNA duplex and 3′ flap site relative to key FEN-1 structural motifs (labeled and color-coded to match Figure 1D) with active site metal ion positions (green spheres) from the *P. furiosus* FEN-1 (PFEN-1) crystal structure (Hosfield et al., 1998b).

(C) Schematic of observed FEN-1:DNA interactions. Hydrogen bonds with DNA involve side chain (red arrows) and backbone atoms (blue arrows). Hydrophobic packing interactions with DNA nucleotides are illustrated with dashed black lines or black arrows.

(D) Sequence, secondary structure, and interface residues of *A. fulgidus* FEN-1 (aFEN-1) aligned with human FEN-1 (hFEN-1). The downstream DNA backbone binding α10-α11 H3TH motif (magenta) and single-strand binding α4-α5 helical clamp (green) are flanked by the DNA 3′ primer binding α2-α3 and α14-α15 motif (red), which is adjacent to the C-terminal PCNA binding motif (gold). Solid dots (•) mark every 10th residue, and asterisks (*) show DNA or PCNA contact residues.

Hwang et al., 1998) reveals conformational changes in the α2-α3 loop that are coupled to increased ordering of the 5′ flap binding α4-α5 helical clamp (Figures 2D and 2E). Concerted shifts of up to 5 Å in the α2-α3 loop (Figures 2D and 2E) appear to be caused by 3′ flap binding (Figure 2E) since they are identical in the two different crystal forms. These DNA-dependent α2-α3 loop movements provide packing interactions with the structurally adjacent α4-α5 helical clamp region that may promote the formation of a well-ordered helical structure, which closes over the active site.

In crystal structures of FEN-1 homologs determined without DNA, the α4-α5 helical clamp region is either completely disordered or adopts drastically different

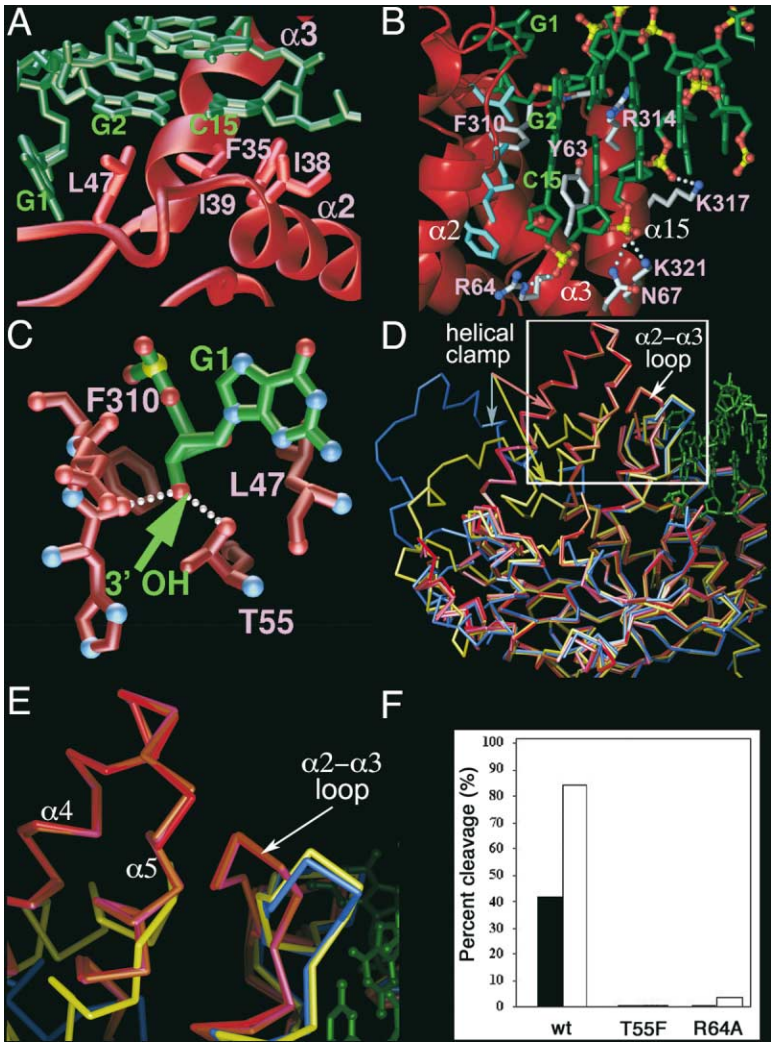

Figure 2. FEN-1 Binds to the 3′ Flap and Promotes Conformational Changes that Facilitate Structure-Specific Catalysis

(A) A hydrophobic wedge (red) formed by Phe35, Ile38, and Ile39 (α3) and Leu47 (α2-α3 loop) opens the dsDNA and stabilizes the terminal base pair of the upstream duplex (G2:C15).

(B) FEN-1 residues (white) from α3 and α15 (red) interact with dsDNA via hydrogen bonding (white dots) to the DNA (green) phosphate backbone, or stacking interactions with sugars in the minor groove (Arg314). A hydrophobic wedge (cyan residues) packs with the terminal base pair (G2:C15).

(C) The 3′ flap (G1: green) binding site is a specific pocket between the α2-α3 and α13-α14 loops (red). Thr55 Oγ and the backbone carbonyl of Phe310 form hydrogen bonds (white dots) with the terminal 3′ hydroxyl of the overhanging 3′ nucleotide.

(D) Superposition of FEN-1 structures from both crystal forms of the aFEN-1:DNA complex (2.0 Å resolution, red; 2.5 Å, orange), with unbound FEN-1 structures from *P. furiosus* (PDB code 1B43, blue) and *M. jannaschii* (PDB code 1A77, yellow), show conserved core structures but significant FEN-1 conformational changes causing interactions between the now ordered α4-α5 helical clamp and the α2-α3 loop.

(E) Conserved shifts in the backbone positions of the α2-α3 loop and α4-α5 helical clamp upon DNA binding occur in both aFEN-1:DNA crystal forms (red, orange) compared to unbound FEN-1 (blue, yellow).

(F) Mutation of residues Thr55 to Phe or Arg64 to Ala almost eliminates enzyme activity against both double-flap (clear bars) and nicked-flap (solid bars) substrates.

conformations (Figure 2D). In contrast, the helical clamp in the FEN-1:DNA structures adopts a well-ordered antiparallel two-helix bundle (Figures 2D and 2E). The predominant α-helical structure of the helical clamp region observed in the FEN-1:DNA cocrystal structure is consistent with biochemical and spectroscopic data that show both conformational changes and an increase in α-helical content upon FEN-1 binding to DNA (Kim et al., 2001). Mutational analyses of residues in this region suggest that conformational flexibility of the helical clamp is important for catalysis (Storici et al., 2002). Together, these data suggest that ordering of the helical clamp region is coupled to FEN-1 conformational changes promoted by the specific recognition of the 3′ flap region of duplex DNA.

FEN-1 Kinks DNA to Facilitate Flap Recognition

To independently define the conformation of a double-flap substrate bound to FEN-1 in solution, we monitored how FEN-1 binding changes the end-to-end distances of fluorescently end-labeled DNA substrates in solution using fluorescence resonance energy transfer (FRET) (Figure 3A; Table 1). By measuring changes in the fluorescence intensity of the rhodamine (acceptor) peak upon excitation of fluorescein (donor), we determined the distance in space between the two dyes in the absence and presence of FEN-1 (Figures 3A and 3B).

To accurately characterize conformational changes in DNA, we performed FRET measurements on three substrates of differing lengths (Table 1). For each substrate, the presence of FEN-1 increases the fluorescence intensity of rhodamine and decreases the fluorescence intensity of fluorescein (Figure 3C; Table 1). The fluorescence intensity of substrates labeled with only fluorescein or rhodamine remains constant and is independent of protein concentration. Also, the addition of FEN-1 does not significantly increase the anisotropy values for fluorescein and rhodamine. Therefore, FEN-1 does not quench the donor or acceptor fluorophores, indicating that the observed changes in fluorescence intensities reflect changes in energy transfer caused by decreasing the end-to-end distance. Also, the binding constants from the FRET titration are consistent with previously published FEN-1 binding assays (Figures 3B) (Friedrich-Heineken et al., 2003). Together, these results suggest that FEN-1 binding to the double-flap substrate

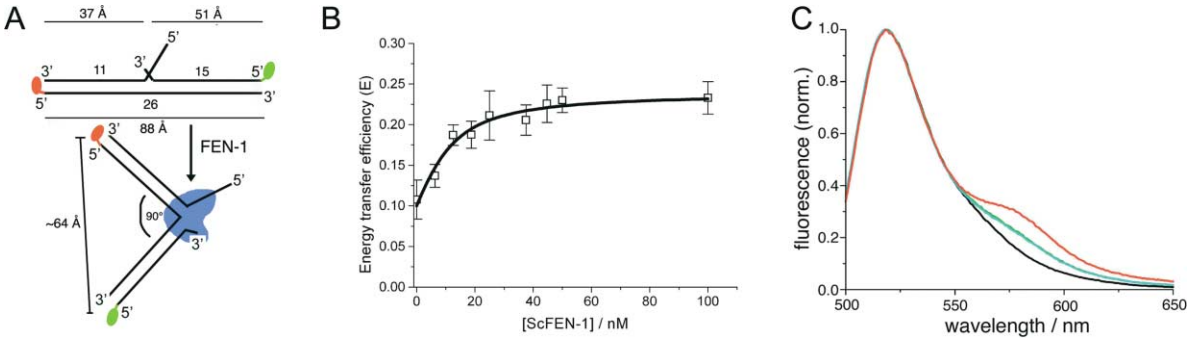

Figure 3. FRET Measurements Define Kinked DNA Binding by FEN-1 in Solution

(A) FRET experiment with expected changes in dye-dye distance caused by FEN-1 binding to DNA.

(B) FEN-1 binding to donor and acceptor-labeled double-flap substrate dsDNA causes a change in FRET efficiency from 0.10 to 0.24, indicating a decrease in the end-to-end distance of the double-labeled DNA consistent with kinking of double-flap DNA.

(C) Solution FRET measurements shown as normalized fluorescence spectra of donor-only (fluorescein) labeled DNA (black), donor (fluorescein)-acceptor (rhodamine) labeled double-flap substrate dsDNA (red), donor-acceptor labeled control dsDNA (blue-green). The addition of 5-fold molar excess FEN-1 protein does not change the spectrum of the donor-acceptor control dsDNA substrate.

causes a major conformational change in the DNA that decreases the distance between the ends of the DNA.

Starting from the FEN-1:DNA cocrystal structure, the decrease in end-to-end distance of the DNA substrate can be explained by a kink centered at the phosphate opposite the flap junction (Figures 3A and 4). The FRET distance measurements support a kink angle of 90°–100° (Table 1), such that the downstream duplex could lie along the positively charged groove (Figures 4A and 4B). The scissile phosphate, located between the first and second downstream nucleotides, is positioned near metal site I, restraining possible rotations of the downstream DNA duplex (Figure 4C). This position of the downstream DNA agrees with biochemically derived models that describe DNA binding by FEN-1 and related 5′ nucleases (Allawi et al., 2003; Dervan et al., 2002). Specifically, the resulting binding orientation suggests that a glycine-rich loop in the H3TH (helix-three turn-helix) motif contacts the phosphate backbone of the template strand in the downstream DNA duplex. These same residues in *P. furiosus* FEN-1 were predicted to contact the same region of DNA based on methyl phosphonate footprinting (Allawi et al., 2003).

The kinked DNA binding mode proposed here for FEN-1 resembles cocrystal structures of gap-filling complexes of polymerase β bound to nicked DNA (Sawaya et al., 1997). Our FEN-1:DNA binding model suggests that additional hydrophobic packing interactions between the first downstream base pair and residues on α2, including conserved Tyr33 and Gln34 (and possibly Ser37 and Ile38), may stabilize the downstream duplex to position the scissile phosphate within the nuclease active site (Figures 4B and 4C).

Two Adjacent but Structurally Distinct Motifs for PCNA Interactions with FEN-1

To examine structural interactions between FEN-1 and PCNA associated with FEN-1 activation, we determined structures of *A. fulgidus* PCNA (aPCNA) alone and in complex with peptides derived from the C terminus of FEN-1 (Supplemental Table S1 on the *Cell* website). The 1.8 Å resolution aPCNA crystal structure without bound

Table 1. Summary of FRET Measurements with Different Length Substrates

	Sample	energy transfer (E)	dye-distance[a] (Å)	predicted dye distance[b] (Å)
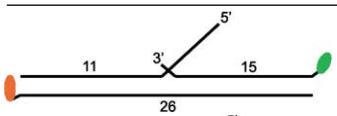	DNA only	0.10 ± 0.01	79 ± 1	88
	DNA+FEN-1	0.24 ± 0.01	67 ± 1	63
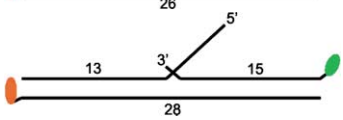	DNA only	0.06 ± 0.01	87 ± 3	95
	DNA+FEN-1	0.21 ± 0.01	69 ± 1	67
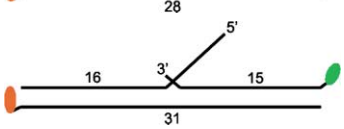	DNA only	0.034 ± 0.01	96 ± 5	105
	DNA+FEN-1	0.146 ± 0.01	73 ± 1	75

[a] The distances were determined from energy transfer efficiencies with Förster (R_0) distance of 55 Å

[b] Calculated distances are based on the length of B-form DNA, accounting for the length of the dye-linker, and helical position of the fluorescently labeled base.

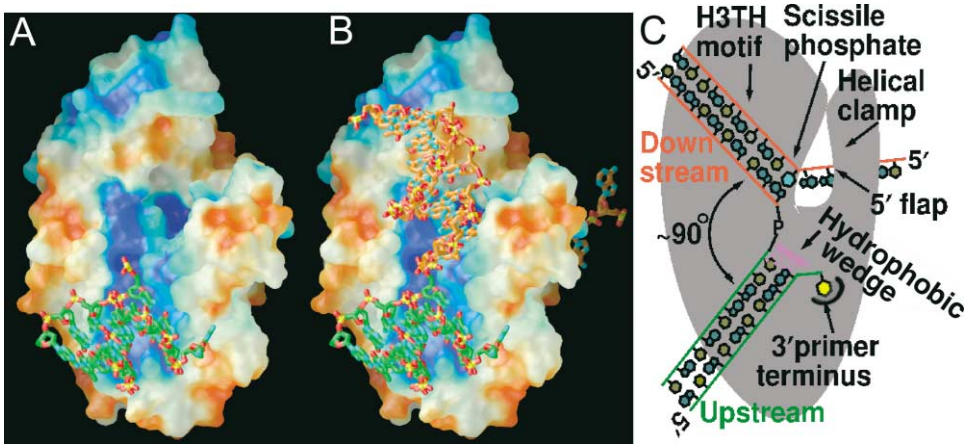

Figure 4. Double-Flap DNA Substrate Binding to FEN-1 Based upon the Electrostatic and Surface Properties of the aFEN-1:DNA Complex

(A) The aFEN-1 solvent-accessible surface and shape of the positively changed groove (blue) with bound 3′ upstream duplex (green bases, yellow phosphates, red oxygens).

(B) Structurally implied docking of the double-flap DNA substrate based on FRET measurements. The double-flap substrate is kinked by ~90° and fits well within the electropositive groove on FEN-1. This binding orientation places the downstream DNA (orange bases) into an electrostatically positive groove to interact with the H3TH and places the 5′ flap in the active site. The 5′ flap may thread through the helical clamp (shown) or track along the clamp (Bornarth et al., 1999; Ceska et al., 1996).

(C) Schematic of FEN-1 with key elements for specific substrate recognition depicted.

peptide establishes the conserved trimeric structure of this toroidal processivity factor, which is consistent with existing crystal structures of PCNA from different organisms (Gulbis et al., 1996; Krishna et al., 1994; Matsumiya et al., 2001). The structures of aPCNA in all the crystal structures are very similar, with less than 1 Å rmsd for all Cα atoms. However, the 2.0 Å and 2.8 Å resolution cocrystal structures of both an aFEN-1 peptide or consensus FEN-1 peptide bound to aPCNA reveal two adjacent but structurally distinct motifs for PCNA interactions with FEN-1 (Figures 5A–5C).

The conserved PCNA binding motif is an eight residue sequence, Q-X-X-(L/I/M)-X-X-(F/Y/W)-(F/Y) (Warbrick, 1998). The C-terminal residues of the FEN-1 peptides (TLERWF/TLDSFF; Figures 5B–5D) adopt a 3_{10} helical conformation and bind within a hydrophobic pocket on PCNA (Figure 5E). Residues from the interdomain connecting loop and nearby β strands form this conserved binding pocket on the PCNA surface (yellow residues, Figure 5B). The interactions of this motif and its structural conservation affirm its role as a hydrophobic anchor to attach replication and repair enzymes to the PCNA trimer. In addition, our structures show that the conserved Gln forms both direct and water-mediated hydrogen bonds suitable to stabilize the base of the PCNA C terminus and the hydrophobic binding pocket (Figures 5A and 5B), consistent with other PCNA:peptide structures (Gulbis et al., 1996; Matsumiya et al., 2002; Shamoo and Steitz, 1999).

In contrast, the peptide residues preceding the conserved PCNA binding motif (KSTQA/KTTQS, Figures 1D and 5D) form an antiparallel β sheet with residues at the C terminus of PCNA (Figures 5A–5C). This β sheet structure causes a significant movement of the C terminus of PCNA, with an average rmsd of 3.5 Å and up to 8 Å shifts between the C-terminal Cα atoms of bound and unbound aPCNA structures. These intermolecular interactions define a conformational change that transforms the open flexible loop seen in the C terminus of the aPCNA structure into an ordered β strand that interacts with a β strand formed by the first six residues of the FEN-1 peptide (Figures 5B and 5C). The resulting antiparallel, intermolecular β sheet structure, which we term a β zipper, points outward, perpendicular to the plane of the PCNA surface (Figure 5E). The topology of this structural interface and its location directly adjacent to the 3′ DNA binding site suggest that β zipper formation may aid in positioning FEN-1 on the PCNA surface.

We tested the biological relevance of the PCNA:FEN-1 peptide interfaces by assaying the ability of aPCNA to stimulate the activity of aFEN-1 and of an aFEN-1 mutant that contains the FEN-1 consensus PCNA binding motif (326-KTTQSTLDSFF-336; Figure 5D). aPCNA stimulates the activity of both enzymes by ~15–20-fold (Figure 5F). Addition of the aFEN-1 peptide to the reaction reduces aPCNA-mediated activity stimulation by ~10-fold (Figure 5F). A nontrimeric aPCNA mutant (Y106A/K107P), similar to the monomeric yeast PCNA mutants S115P (Ayyagari et al., 1995) and Y114A (Jonsson et al., 1995), does not stimulate FEN-1 activity, indicating that aPCNA must be encircling DNA in order to stimulate FEN-1 activity.

Despite their sequence differences, both FEN-1-derived peptides adopt nearly identical conformations and can be superimposed with an rmsd of 0.5 Å for all peptide Cα atoms. When the PCNA structures are aligned based only on PCNA atoms, the peptides differ by an rmsd of 1.4 Å for all Cα atoms, caused by a slight uniform shift of the β zipper region (Figure 5C). New studies of a bacterial PolIV domain support an analogous β sheet interface formed between PolIV and the β clamp in *E. coli* (Bunting et al., 2003), consistent with our structural, biochemical, and mutational results on archaeal and eukaryotic PCNA:FEN-1 interfaces. Given

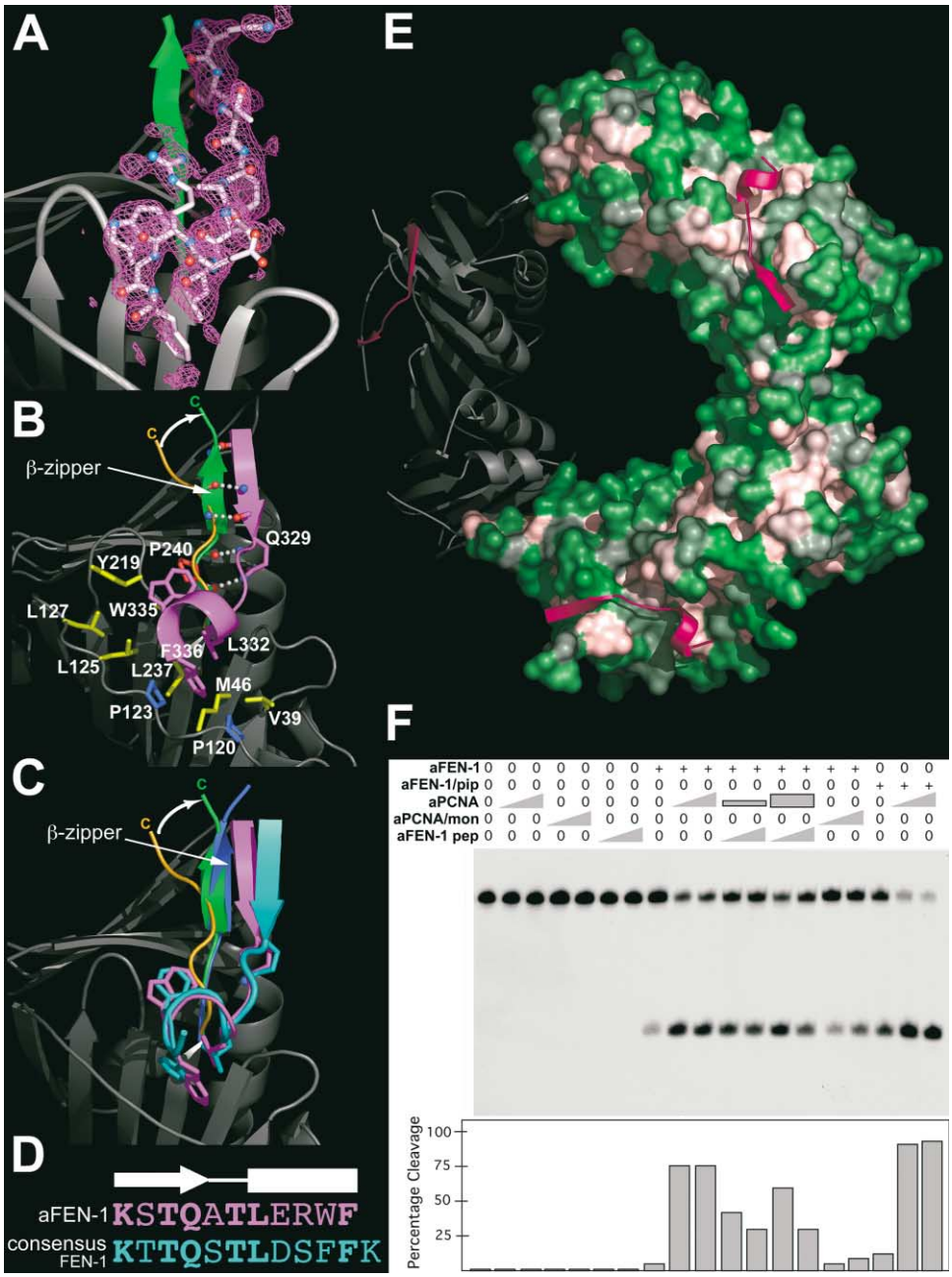

Figure 5. β Zipper Formation at the FEN-1:PCNA Binding Interface and PCNA Stimulation of FEN-1 Activity

(A) The σ_A-weighted $2F_o$-F_c electron density (magenta, 1.5 σ) for the aFEN-1 peptide (white) bound to aPCNA (cyan and green) shows that the peptide is well ordered in the cocrystal structure.

(B) Binding of the aFEN-1-peptide (magenta) to PCNA forms a β zipper interface that transforms the unstructured C terminus of PCNA (orange) into an ordered, antiparallel β strand (green) that forms main chain hydrogen bonds (white spheres) with the N terminus of the aFEN-1 peptide (magenta). In yeast, mutation of Pro240 (red), located at the base of the β zipper, prevents FEN-1 interaction with PCNA bound DNA. The C terminus of the peptide forms a 3_{10} helix, allowing conserved residues (magenta residues) to bind a hydrophobic cavity on PCNA (yellow residues). In yeast and human PCNA, mutation of hydrophobic residues at the positions of Pro120 and Pro123 (blue) disrupts bimolecular interaction between FEN-1 and PCNA in the absence of DNA.

(C) Comparison of all three aPCNA structures, superimposed based on all Cα atoms of aPCNA. The aFEN-1 peptide (magenta) and the consensus FEN-1 peptide (cyan) both adopt the same structure. The C terminus of aPCNA transforms from an unstructured loop (unbound aPCNA, orange) to an ordered β sheet with the C terminus of aPCNA (aPCNA:aFEN-1 peptide, green; aPCNA:consensus FEN-1 peptide, blue).

(D) The sequence and secondary structures of the aFEN-1 peptide (magenta) and the consensus FEN-1 peptide (cyan). Identical residues are highlighted in bold.

(E) The molecular surface of the aPCNA trimer colored by hydrophobicity (white = hydrophobic; green = hydrophilic) shows how the aFEN-1:peptide (magenta) interacts with aPCNA. The helical region of the peptide interacts with a hydrophobic patch, while the N terminus of the peptide forms a β sheet with the C terminus of aPCNA, which points out and away from the surface.

(F) aPCNA stimulates the activity of both aFEN-1 and an aFEN-1 mutant that contains the consensus PCNA binding motif (aFEN-1/pip-mut) by 15- to 20-fold. The peptide derived from aFEN-1 (KSTQATLERWF, aFEN-1 pep) inhibits aPCNA-dependent stimulation by ~10-fold. A monomeric mutant of aPCNA (aPCNA/mon) does not stimulate FEN-1 activity, indicating that aPCNA must be encircling DNA in order to stimulate FEN-1 activity.

the role of the C terminus of PCNA in other DNA metabolic pathways, the intermolecular β zipper may be a conserved structural interface among enzyme:PCNA complexes.

Discussion

FEN-1 Substrate Recognition and Catalysis

The FEN-1:DNA complex structures imply a direct link between 3′ flap binding and conformational ordering of the helical clamp. We propose that FEN-1 binding to the 3′ flap, in addition to hydrophobic contacts with the exposed bases, anchors the DNA in a defined orientation. The structural and FRET results suggest that the DNA is kinked, such that when the 3′ flap is bound, the scissile phosphate is positioned near the active site. Because of the 25 Å separation between the 3′ flap binding site and the active site, FEN-1 could track along the 5′ flap, but not efficiently catalyze phosphodiester cleavage until 3′ flap binding promotes ordering of the helical clamp over the properly positioned substrate. The results presented here argue that 3′ flap binding defines a registration point that may provide a "molecular ruler" to ensure that the scissile phosphate is positioned near the active site. Binding of the 3′ flap could then promote closing of an ordered, helical clamp over the active site. This DNA-dependent, conformational change would exclude bulk solvent from the active site and facilitate precise cleavage of the substrate at the base preceding the flap junction.

A Molecular Mechanism for PCNA Stimulation of FEN-1 Activity

The FEN-1 peptide:PCNA structure suggests that PCNA may regulate FEN-1 activity by structurally ordering FEN-1 residues linking the PCNA binding motif to a DNA binding region. The structural, biochemical, and mutational results presented here show that residues from the unstructured C termini of PCNA and FEN-1 interact to form ordered β strands, creating an intermolecular β zipper interface (Figures 5B and 5C). The FEN-1 residues involved in β zipper formation link a DNA binding helix (α15, Figure 2B) to the PCNA binding hydrophobic anchor motif (Figures 5B and 5D). Thus, the β zipper residues directly connect motifs that contact DNA and PCNA (Figures 1B and 1D). We propose that β zipper formation may functionally enhance FEN-1 binding to DNA via the α14-α15 region and restrain the orientation of FEN-1 relative to PCNA bound DNA. Thus, we argue that β zipper formation likely explains the observed decrease in K_m for FEN-1 activity in the presence of PCNA (Tom et al., 2000).

Since β sheet formation depends primarily on peptide backbone hydrogen bonds, the β zipper interface formed by FEN-1 and PCNA residues should be largely independent of the protein sequence. This observation is consistent with the otherwise surprising demonstration that PCNA can stimulate FEN-1 activity even when all of the residues in the PCNA binding motif of FEN-1 are mutated to alanine (Frank et al., 2001). Yet, in apparent conflict with our proposal, mutation of two conserved C-terminal β zipper residues in yeast PCNA (Pol30, P252A, K253A; Figure 5B, red residues) significantly reduces the ability of FEN-1 to interact with PCNA on DNA (Gomes and Burgers, 2000). However, our structures argue that this conserved proline (yeast PCNA Pro252, aPCNA Pro240), which is located at the base of the β zipper, acts as a rigid joint that directs the β zipper out and away from the PCNA surface. While other amino acids might satisfy the phi-psi requirements at this position, the rigid backbone of proline may ensure proper β zipper formation by preventing the C terminus of PCNA from forming stable interactions with other PCNA residues. Thus, the existing mutational studies on the PCNA C terminus appear to support the proposal of its role in FEN-1 activation.

The β zipper formed between FEN-1 and the C terminus of PCNA appears to be a functionally important, previously uncharacterized structural motif for interaction with PCNA. However, similar interactions with the C terminus of PCNA may control enzyme interactions and activities in other pathways, such as mismatch repair. Msh6p and Msh3p both contain PCNA interaction motifs, and genetic data suggest that the C terminus of PCNA is critical for supporting mismatch repair (Eissenberg et al., 1997; Johnson et al., 1996). Since similar PCNA interactions may control different pathways, our results characterizing this interface for PCNA:FEN-1 interactions provide a model system for understanding how dynamic components assemble into precisely aligned complexes to regulate enzymatic activities in other pathways.

PCNA Coordination during DNA Replication and Repair

The conformational changes defined here for FEN-1:DNA and FEN-1:PCNA interactions provide a specific structural basis whereby PCNA may enhance the efficiency of bound enzymes. Docking our aFEN-1:DNA structure onto our aPCNA:FEN-1-peptide complex (Figure 6A) also supports a specific model for FEN-1 localization at the DNA replication and repair locus. The composite model positions the nuclease on the polymerase binding, front face of PCNA, with the upstream duplex DNA protruding through the central cavity of PCNA and the downstream DNA kinked ~90°, orthogonal to the upstream duplex (Figure 6A). The FEN-1 hydrophobic wedge opens the DNA helix, enforcing a kink that facilitates 3′ and 5′ flap recognition. This kinked DNA conformation may be a feature of other PCNA complexes. For example, the gap-filling complexes of polymerase β (Sawaya et al., 1997), which is known to bind PCNA (Kedar et al., 2002), show a kinked DNA topology that facilitates DNA end discrimination. The structure of the NAD^+-dependent DNA ligase from *T. filiformis* (Lee et al., 2000) also suggests that an ~90° DNA kink is important for nick recognition. Thus, DNA polymerase, FEN-1, and DNA ligase may all recognize a sharply kinked DNA substrate localized on PCNA.

Recognition of a common kinked substrate is consistent with previously proposed models for the transition of Taq polymerase from DNA polymerase activity to 5′ nuclease (FEN-1) activity. These studies suggest that the 5′ nuclease domain (homologous to FEN-1) binds the 3′ flap generated by DNA polymerase during displacement synthesis, halting polymerization and stimu-

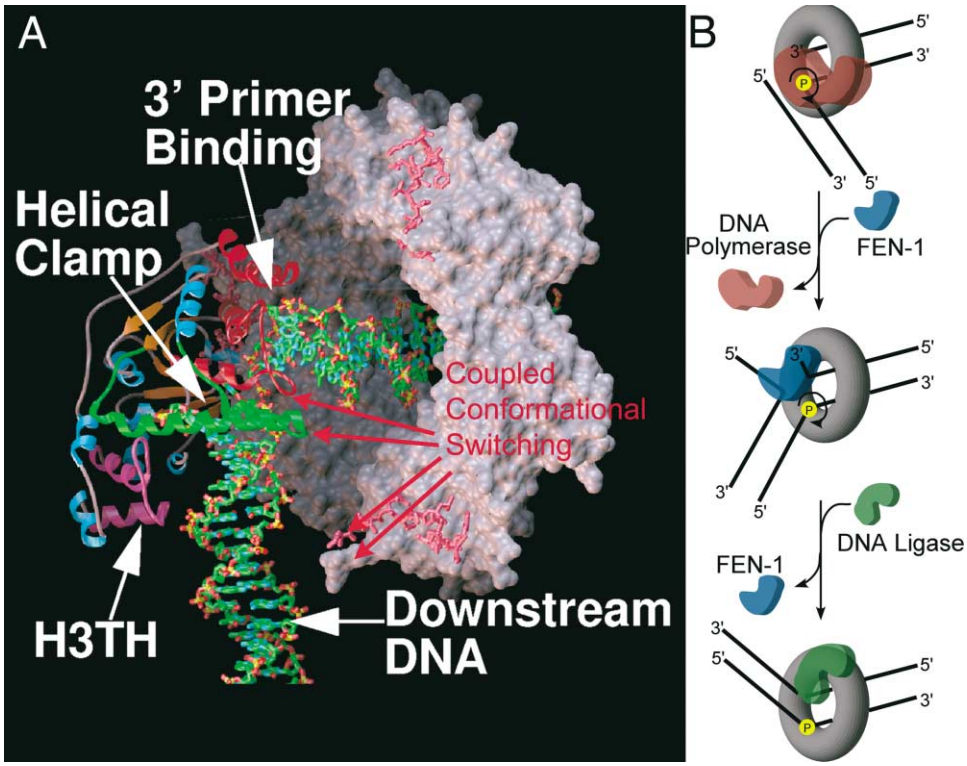

Figure 6. Composite Structure of the aFEN-1:DNA and FEN-1 Peptide:aPCNA Complexes Suggests a PCNA-Coordinated Rotary Handoff Mechanism

(A) The composite structure of the aFEN-1:DNA and FEN-1-peptide:aPCNA complexes places the downstream duplex (vertical) through the central cavity of PCNA with the upstream duplex (horizontal) kinked ~90° by FEN-1. Conformational changes in the α2-α3 loop and helical clamp of FEN-1 coupled to intermolecular β zipper formation between FEN-1 and PCNA residues suggest how association with PCNA stimulates FEN-1 catalysis. DNA polymerase and DNA ligase could conceivably either occupy or sequentially bind the two additional binding sites on the PCNA trimer (identified by the bound peptide, pink).

(B) A rotary-handoff model suggests how PCNA (gray torus) might coordinate the sequential activities of DNA polymerase β/δ/ϵ (brown), FEN-1 (blue), and DNA ligase I (green) during DNA replication and repair. Since each enzyme can potentially recognize a kinked DNA intermediate (black lines), rotation about the phosphate bond (P, yellow sphere) at the vertex of the kink could facilitate the sequential handoff of DNA intermediates at the PCNA locus.

lating cleavage of the 5′ flap (Kaiser et al., 1999; Maga et al., 2001). The recent findings that polymerase β binds to PCNA via a sequence similar to the conserved PCNA interaction motif (Kedar et al., 2002) and can participate in long-patch base-excision repair prior to FEN-1 activity (Klungland and Lindahl, 1997) suggest that recognition of a kinked DNA structure could facilitate transfer of DNA from polymerase β to FEN-1 at the PCNA locus (Figure 6B).

Taken together, the results presented here identify FEN-1:DNA and FEN-1:PCNA binding interfaces and motifs that become ordered upon complex formation. These results suggest how FEN-1 acts as a structure-specific endonuclease and how PCNA stimulates FEN-1 activity. The open, kinked forms of DNA bound by FEN-1 and polymerase β may allow rotations of DNA substrates about the DNA phosphate bond opposite the 3′ flap. Rotation of the kinked DNA substrate would allow enzymes bound at any of the three binding sites on the PCNA trimer to access the kinked DNA intermediate (Figure 6B). This observation suggests a possible PCNA-mediated, rotary-handoff mechanism (Figure 6B). For the analogous bacterial system, the recent structure of an *E. coli* PolIV domain bound to the β clamp implies two binding states: a "locked-down," inactive state and an active, "tethered" state that are controlled by the extent of interaction with the β clamp (Bunting et al., 2003). Such active and inactive conformations for enzymes bound to PCNA are consistent with our proposal that the formation of protein:protein interfaces provides a mechanism for PCNA to regulate and coordinate sequential enzyme activities. Regardless of the precise molecular mechanism, the structural interfaces and transitions identified here support the dynamic assembly of FEN-1, DNA, and PCNA into a conformationally restricted and aligned complex. These interfaces thus provide a molecular basis for PCNA regulation of FEN-1 activity and suggest how similar interactions with PCNA may promote the coordination of enzymatic activities during DNA replication and repair.

Experimental Procedures

Protein Expression and Purification

Expression and purification of *Archaeoglobus fulgidus* FEN-1 (aFEN-1), aFEN-1 mutants, and *Saccharomyces cerevisiae* Rad27p followed published methods (Frank et al., 2001; Hosfield et al., 1998a). Cloning, expression, and purification of *A. fulgidus* PCNA

(aPCNA) used similar protocols (see Supplemental Data on *Cell* website for details).

Crystallization and Data Collection

aFEN-1 (25 mg/ml) was mixed with an equal volume of ~2 mM upstream primer duplex DNA containing a 3′ flap (upstream primer 5′-TAGCATCGG; template 5′-CGATGCTA) and incubated at room temperature for 60 min. The aFEN-1:DNA complex was crystallized in space group $P4_12_12$, with cell dimensions a = b = 87, c = 251 Å and two molecules in the asymmetric unit, by vapor diffusion at 21°C after mixing with an equal volume of precipitant solution (5% MPEG 5000, 100 mM sodium acetate. pH 4.8, and 5% ethylene glycol). The aFEN-1:DNA complex was also crystallized in space group $P2_12_12$, with cell dimensions a = 44, b = 86, c = 109 Å, by the same method using a precipitant solution containing 15% PEG4000, 100 mM NH_4SO_4, and 15% glycerol.

aPCNA was crystallized in space group $F4_132$, with cell dimensions a = b = c = 244 Å, by vapor diffusion at 21°C after mixing equal volumes of aPCNA (25 mg/ml, 50 mM Tris, pH 8.0, 250 mM NaCl) with precipitant (1.4–1.6 M Na/K phosphate, pH 9.0). aPCNA:peptide complexes were formed by mixing equal volumes of 0.9 mM aPCNA with 1 mM consensus FEN-1 peptide (KTTQSTLDSFFK) or 2.4 mM aPCNA with 2.7 mM of aFEN-1 peptide (KSTQATLERWF). The aPCNA:(consensus FEN-1 peptide) complex was crystallized in space group R32, with cell dimensions a = b = 101, c = 203 Å, using the same method and conditions used for aPCNA. The aPCNA:(aFEN-1 peptide) complex was crystallized in space group R3, with cell dimensions a = b = 86, c = 97 Å, by the same method and conditions used for aPCNA.

All X-ray diffraction data were measured from single crystals cooled to 100 K at either the Advanced Photon Source (APS), the Advanced Light Source (ALS), or the Stanford Synchrotron Radiation Laboratory (SSRL) (see Supplemental Data online for details).

Structure Determination and Refinement

The aFEN-1:DNA structure was determined to 2.5 Å by MAD phasing. Phases for the 1.9 Å data were determined by molecular replacement (see Supplemental Data). The current model has an R factor of 0.242 (R_{free} = 0.278).

The initial structure of aPCNA was determined to 1.8 Å resolution by analysis of the native data merged with a single isomorphous mercury derivative. The current model has been refined to an R factor of 0.219 (R_{free} = 0.238) (Supplemental Table S1). Both aPCNA:peptide structures were determined by molecular replacement using aPCNA as a search model. The current model for the PCNA:(consensus FEN-1 peptide) was refined to an R factor of 0.205 (R_{free} = 0.261) (Supplemental Table S1). Refinement of the PCNA:(aFEN-1 peptide) complex was complicated due to the fact that the data were merohedrally twinned with a twinning operator of h,-h-k,-l and a twin fraction of 0.37. Refinement of this data in CNS produced reasonable refinement statistics (Supplemental Data). The current twinned R factor for this structure is 0.19 (R_{free} = 0.26) (Supplemental Table S1).

Fluorescence Resonance Energy Transfer (FRET)

Synthetic deoxyoligonucleotides labeled on the 5′ end with either fluorescein (6-FAM) or rhodamine (TAMRA) were purchased from Midland Certified Reagent Co. and purified by 20% polyacrylamide/7M urea gel electrophoresis. Complementary oligos (templatetamra: 5′ (TAMRA)-TGGACGGGTGGCGTTAAGGTTAGGCT; 3flap15-fam: 5′-(6-FAM)AGCCTAACCTTAACGG; 5flap4: 5′-TTTTCCACCC GTCCA) were annealed by slow cooling in 50 mM NaCl, 10 mM Tris, pH 8.0), purified by native polyacrylamide gel electrophoresis (PAGE), and recovered by soaking in complexation buffer (10 mM Tris, pH 8.0, 10 mM NaCl, 5 mM EDTA, 10% glycerol). A fixed amount (10 nM) of double-labeled, donor-only labeled, or acceptor-only labeled DNA was titrated with yeast FEN-1 and incubated for 5 min at room temperature in complexation buffer. Yeast FEN-1 was used for FRET experiments to ensure rapid binding at the temperatures required for substrate stability. Steady-state fluorescence spectra were taken on a Fluoromax-3 (Horiba/Yobin-Yvon) and corrected for lamp and wavelength variations. Fluorescence spectra were collected over a range of emission wavelengths, corrected for buffer background signal (FRET signal, λ_{ex} = 490 nm, λ_{em} = 500–650 nm; acceptor signal, λ_{ex} = 560 nm, λ_{em} = 570–650 nm), and processed using the program GRAMS/32 (Galactic Ind., New Hampshire). The sensitized acceptor emission due to FRET was determined by the $ratio_A$ method (Clegg, 1992). The Förster distance (R_0) for this dye pair was calculated to be 55 Å and was used in combination with measured energy transfer efficiencies (E) to calculate the distance (R) between dye pairs ($E = R_0^6/[R_0^6 + R^6]$). DNA bending angles were calculated based on the length of double-stranded B form DNA, the length of the dye linker, and the helical position of the fluorescently labeled base using previously described helical models for nucleic acids (Clegg et al., 1993), assuming that the vertex of the bend was positioned at the phosphate opposite the nick.

FEN-1 Activity Assays

Wild-type and site-directed mutants of aFEN1 (Thr55Phe or Arg64Ala) (40 nM) were incubated with 120 nM of either a nicked-flap substrate (Hosfield et al., 1998a) or a double-flap substrate (Qiu et al., 2002) in a total volume of 15 μl with buffer (50 mM Tris, pH 8, 10 mM $MgCl_2$, 50 μg/mL BSA) for 15 min. Reactions were stopped, and products were analyzed according to published procedures (Hosfield et al., 1998a; Qiu et al., 2002).

DNA Substrate Preparation and FEN-1 Nuclease Activity Stimulation Assays

The double-flap substrate was formed by annealing 40 pmol of afSUB-FLAP (5′-AAAAAAAAACGCTGTCTCGCT-3′) with 80 pmol afSUB-C (5′-AGCGAGACAGCGACAGACGCTCGT-3′) and 80 pmol afSUB-P_0 (5′-ACGAGCGTCTGT-3′) and end-labeled as described (Qiu et al., 2002). Reactions used the indicated amount of aFEN-1 and aPCNA proteins (1.36 pmol of aFEN-1 or its mutant, aFEN-1- pip mut; 8 or 16 pmol of aPCNA or aPCNA y106a, K107p; and 16 or 32 pmol of the peptide, Pip) and 800 fmol of flap substrate in reaction buffer containing 50 mM Tris (pH 8.0) and 10 mM $MgCl_2$ in a total volume of 10 μl. All reactions were incubated at 50°C for 20 min and terminated by adding an equal volume of stop solution (95% formamide, 20 mM EDTA, 0.05% bromophenol blue, 0.05% xylene cyanol). Reaction products were analyzed as described previously (Qiu et al., 2002).

Acknowledgments

We thank S.G. Zeitlin, C.D. Mol, E.D. Garcin, and D.P. Millar for helpful discussion; S.S. Parikh for data collection assistance; F. Henderson for technical assistance; and staff at ALS, APS, and SSRL for key synchtron facilities. This work was supported by National Cancer Institute grants (CA081967 and P01 CA92584 to J.A.T.), Graduate Fellowships from the Skaggs Institute for Chemical Biology (B.R.C. and D.J.H.), and an NSF graduate research fellowship (B.R.C.).

Received: July 14, 2003
Revised: December 15, 2003
Accepted: December 16, 2003
Published: January 8, 2004

References

Allawi, H.T., Kaiser, M.W., Onufriev, A.V., Ma, W.P., Brogaard, A.E., Case, D.A., Neri, B.P., and Lyamichev, V.I. (2003). Modeling of flap endonuclease interactions with DNA substrate. J. Mol. Biol. *328*, 537–554.

Ayyagari, R., Impellizzeri, K.J., Yoder, B.L., Gary, S.L., and Burgers, P.M. (1995). A mutational analysis of the yeast proliferating cell nuclear antigen indicates distinct roles in DNA replication and DNA repair. Mol. Cell. Biol. *15*, 4420–4429.

Bambara, R.A., Murante, R.S., and Henricksen, L.A. (1997). Enzymes and reactions at the eukaryotic DNA replication fork. J. Biol. Chem. *272*, 4647–4650.

Bornarth, C.J., Ranalli, T.A., Henricksen, L.A., Wahl, A.F., and Bambara, R.A. (1999). Effect of flap modifications on human FEN1 cleavage. Biochemistry *38*, 13347–13354.

Bunting, K.A., Roe, S.M., and Pearl, L.H. (2003). Structural basis

for recruitment of translesion DNA polymerase Pol IV/DinB to the β-clamp. EMBO J. *22*, 5883–5892.

Ceska, T.A., Sayers, J.R., Stier, G., and Suck, D. (1996). A helical arch allowing single-stranded DNA to thread through T5 5′-Exonuclease. Nature *382*, 90–93.

Clegg, R.M. (1992). Fluorescence resonance energy transfer and nucleic acids. Methods Enzymol. *211*, 353–388.

Clegg, R.M., Murchie, A.I., Zechel, A., and Lilley, D.M. (1993). Observing the helical geometry of double-stranded DNA in solution by fluorescence resonance energy transfer. Proc. Natl. Acad. Sci. USA *90*, 2994–2998.

Dervan, J.J., Feng, M., Patel, D., Grasby, J.A., Artymiuk, P.J., Ceska, T.A., and Sayers, J.R. (2002). Interactions of mutant and wild-type flap endonucleases with oligonucleotide substrates suggest an alternative model of DNA binding. Proc. Natl. Acad. Sci. USA *99*, 8542–8547.

Eissenberg, J.C., Ayyagari, R., Gomes, X.V., and Burgers, P.M. (1997). Mutations in yeast proliferating cell nuclear antigen define distinct sites for interaction with DNA polymerase delta and DNA polymerase epsilon. Mol. Cell. Biol. *17*, 6367–6378.

Frank, G., Qiu, J., Zheng, L., and Shen, B. (2001). Stimulation of eukaryotic flap endonuclease-1 activities by proliferating cell nuclear antigen (PCNA) is independent of its in vitro interaction via a consensus PCNA binding region. J. Biol. Chem. *276*, 36295–36302.

Friedrich-Heineken, E., Henneke, G., Ferrari, E., and Hubscher, U. (2003). The acetylatable lysines of human Fen1 are important for endo- and exonuclease activities. J. Mol. Biol. *328*, 73–84.

Gomes, X.V., and Burgers, P.M. (2000). Two modes of FEN1 binding to PCNA regulated by DNA. EMBO J. *19*, 3811–3821.

Gulbis, J.M., Kelman, Z., Hurwitz, J., O'Donnell, M., and Kuriyan, J. (1996). Structure of the C-terminal region of p21(WAF1/CIP1) complexed with human PCNA. Cell *87*, 297–306.

Harrington, J.J., and Lieber, M.R. (1994). Functional domains within FEN-1 and RAD2 define a family of structure-specific endonucleases: Implications for nucleotide excision repair. Genes Dev. *8*, 1344–1355.

Henneke, G., Friedrich-Heineken, E., and Hubscher, U. (2003). Flap endonuclease 1: a novel tumour suppresser protein. Trends Biochem. Sci. *28*, 384–390.

Hosfield, D.J., Frank, G., Weng, Y., Tainer, J.A., and Shen, B. (1998a). Newly discovered archaebacterial flap endonucleases show a structure-specific mechanism for DNA substrate binding and catalysis resembling human flap endonuclease-1. J. Biol. Chem. *273*, 27154–27161.

Hosfield, D.J., Mol, C.D., Shen, B., and Tainer, J.A. (1998b). Structure of the DNA repair and replication endonuclease and exonuclease FEN-1: coupling DNA and PCNA binding to FEN-1 activity. Cell *95*, 135–146.

Hwang, K.Y., Baek, K., Kim, H.Y., and Cho, Y. (1998). The crystal structure of flap endonuclease-1 from *Methanococcus jannaschii*. Nat. Struct. Biol. *5*, 707–713.

Johnson, R.E., Kovvali, G.K., Guzder, S.N., Amin, N.S., Holm, C., Habraken, Y., Sung, P., Prakash, L., and Prakash, S. (1996). Evidence for involvement of yeast proliferating cell nuclear antigen in DNA mismatch repair. J. Biol. Chem. *271*, 27987–27990.

Jonsson, Z.O., Hindges, R., and Hubscher, U. (1998). Regulation of DNA replication and repair proteins through interaction with the front side of proliferating cell nuclear antigen. EMBO J. *17*, 2412–2425.

Jonsson, Z.O., Podust, V.N., Podust, L.M., and Hubscher, U. (1995). Tyrosine 114 is essential for the trimeric structure and the functional activities of human proliferating cell nuclear antigen. EMBO J. *14*, 5745–5751.

Kaiser, M.W., Lyamicheva, N., Ma, W., Miller, C., Neri, B., Fors, L., and Lyamichev, V.I. (1999). A comparison of eubacterial and archaeal structure-specific 5′-exonucleases. J. Biol. Chem. *274*, 21387–21394.

Kao, H.I., Henricksen, L.A., Liu, Y., and Bambara, R.A. (2002). Cleavage specificity of *Saccharomyces cerevisiae* flap endonuclease 1 suggests a double-flap structure as the cellular substrate. J. Biol. Chem. *277*, 14379–14389.

Kedar, P.S., Kim, S.J., Robertson, A., Hou, E., Prasad, R., Horton, J.K., and Wilson, S.H. (2002). Direct interaction between mammalian DNA polymerase beta and proliferating cell nuclear antigen. J. Biol. Chem. *277*, 31115–31123.

Kim, Y., Eom, S.H., Wang, J., Lee, D.S., Suh, S.W., and Steitz, T.A. (1995). Crystal structure of *Thermus aquaticus* DNA polymerase. Nature *376*, 612–616.

Kim, C.Y., Park, M.S., and Dyer, R.B. (2001). Human flap endonuclease-1: conformational change upon binding to the flap DNA substrate and location of the Mg^{2+} binding site. Biochemistry *40*, 3208–3214.

Klungland, A., and Lindahl, T. (1997). Second pathway for completion of human DNA base excision-repair: reconstitution with purified proteins and requirement for DNase IV (FEN1). EMBO J. *16*, 3341–3348.

Krishna, T.S., Kong, X.P., Gary, S., and Kuriyan, J. (1994). Crystal structure of the eukaryotic DNA polymerase processivity factor PCNA. Cell *79*, 1233–1243.

Kucherlapati, M., Yang, K., Kuraguchi, M., Zhao, J., Lia, M., Heyer, J., Kane, M.F., Fan, K., Russell, R., Brown, A.M., et al. (2002). Haploinsufficiency of flap endonuclease (FEN-1) leads to rapid tumor progression. Proc. Natl. Acad. Sci. USA *99*, 9924–9929.

Lee, J.Y., Chang, C., Song, H.K., Moon, J., Yang, J.K., Kim, H.K., Kwon, S.T., and Suh, S.W. (2000). Crystal structure of NAD(+)-dependent DNA ligase: modular architecture and functional implications. EMBO J. *19*, 1119–1129.

Li, X., Li, J., Harrington, J., Lieber, M.R., and Burgers, P.M. (1995). Lagging strand DNA synthesis at the eukaryotic replication fork involves binding and stimulation of FEN-1 by proliferating cell nuclear antigen. J. Biol. Chem. *270*, 22109–22112.

Lieber, M.R. (1997). The FEN-1 family of structure-specific nucleases in eukaryotic DNA replication, recombination and repair. Bioessays *19*, 233–240.

Maga, G., Villani, G., Tillement, V., Stucki, M., Locatelli, G.A., Frouin, I., Spadari, S., and Hubscher, U. (2001). Okazaki fragment processing: modulation of the strand displacement activity of DNA polymerase delta by the concerted action of replication protein A, proliferating cell nuclear antigen, and flap endonuclease-1. Proc. Natl. Acad. Sci. USA *98*, 14298–14303.

Matsui, E., Musti, K.V., Abe, J., Yamasaki, K., Matsui, I., and Harata, K. (2002). Molecular structure and novel DNA binding sites located in loops of flap endonuclease-1 from Pyrococcus horikoshii. J. Biol. Chem. *277*, 37840–37847.

Matsumiya, S., Ishino, Y., and Morikawa, K. (2001). Crystal structure of an archaeal DNA sliding clamp: proliferating cell nuclear antigen from *Pyrococcus furiosus*. Protein Sci. *10*, 17–23.

Matsumiya, S., Ishino, S., Ishino, Y., and Morikawa, K. (2002). Physical interaction between proliferating cell nuclear antigen and replication factor C from Pyrococcus furiosus. Genes Cells *7*, 911–922.

Matsumoto, Y. (2001). Molecular mechanism of PCNA-dependent base excision repair. Prog. Nucleic Acid Res. Mol. Biol. *68*, 129–138.

Mossi, R., and Hubscher, U. (1998). Clamping down on clamps and clamp loaders–the eukaryotic replication factor C. Eur. J. Biochem. *254*, 209–216.

Mueser, T.C., Nossal, N.G., and Hyde, C.C. (1996). Structure of bacteriophage T4 RNase H, a 5′ to 3′ RNA-DNA and DNA-DNA exonuclease with sequence similarity to the RAD2 family of eukaryotic proteins. Cell *85*, 1101–1112.

Qiu, J., Bimston, D.N., Partikian, A., and Shen, B. (2002). Arginine residues 47 and 70 of human flap endonuclease-1 are involved in DNA substrate interactions and cleavage site determination. J. Biol. Chem. *277*, 24659–24666.

Reynaldo, L.P., Vologodskii, A.V., Neri, B.P., and Lyamichev, V.I. (2000). The kinetics of oligonucleotide replacements. J. Mol. Biol. *297*, 511–520.

Sawaya, M.R., Prasad, R., Wilson, S.H., Kraut, J., and Pelletier, H. (1997). Crystal structure of human DNA polymerase β complexed

with gapped and nicked DNA: Evidence for an induced fit mechanism. Biochemistry *36*, 11205–11215.

Shamoo, Y., and Steitz, T.A. (1999). Building a replisome from interacting pieces: sliding clamp complexed to a peptide from DNA polymerase and a polymerase editing complex. Cell *99*, 155–166.

Shen, B., Qui, J., Hosfield, D.J., and Tainer, J.A. (1998). Flap endonuclease homologues identified in archaebacteria exist as independent proteins. Trends Biochem. Sci. *23*, 171–173.

Storici, F., Henneke, G., Ferrari, E., Gordenin, D.A., Hubscher, U., and Resnick, M.A. (2002). The flexible loop of human FEN1 endonuclease is required for flap cleavage during DNA replication and repair. EMBO J. *21*, 5930–5942.

Tom, S., Henricksen, L.A., and Bambara, R.A. (2000). Mechanism whereby proliferating cell nuclear antigen stimulates flap endonuclease 1. J. Biol. Chem. *275*, 10498–10505.

Warbrick, E. (1998). PCNA binding through a conserved motif. Bioessays *20*, 195–199.

Xie, Y., Liu, Y., Argueso, J.L., Henricksen, L.A., Kao, H.I., Bambara, R.A., and Alani, E. (2001). Identification of rad27 mutations that confer differential defects in mutation avoidance, repeat tract instability, and flap cleavage. Mol. Cell. Biol. *21*, 4889–4899.

Yao, N., Turner, J., Kelman, Z., Stukenberg, P.T., Dean, F., Shechter, D., Pan, Z.Q., Hurwitz, J., and O'Donnell, M. (1996). Clamp loading, unloading and intrinsic stability of the PCNA, beta and gp45 sliding clamps of human, *E. coli* and T4 replicases. Genes Cells *1*, 101–113.

Accession Numbers

Coordinates are deposited with the RCSB Protein Data Bank with accession codes 1RWZ for aPCNA, 1RXM for the aPCNA:(consensus FEN-1 peptide) complex, 1RXZ for the aPCNA:(aFEN-1 peptide) complex, 1RXW for the 2.0 Å aFEN-1:DNA complex, and 1RXV for the 2.5 Å aFEN-1:DNA complex.